Supplementary material for "Transferable diversity – a data-driven representation of chemical space"

Tim Gould,[1] Bun Chan,[2] Stephen G. Dale,[1,3] and Stefan Vuckovic[4]

[1)] *Queensland Micro- and Nanotechnology Centre, Griffith University, Nathan, Qld 4111, Australia*

[2)] *Graduate School of Engineering, Nagasaki University, Bunkyo 1-14, Nagasaki 852-8521, Japan*

[3)] *Institute of Functional Intelligent Materials, National University of Singapore, 4 Science Drive 2, Singapore 117544*

[4)] *Department of Chemistry, University of Fribourg, Fribourg, Switzerland.*[a)]

[a)]Electronic mail: stefan.vuckovic@unifr.ch

CONTENTS

S1. COMPUTATIONAL DETAILS

All unrestricted HF/DFT calculations have been performed from the Orca 5.0.0 package within the def2-QZVPPD basis set for GMTKN55 subsets and def2-QZVP for TMC151 subset. For a small number of reactions when this basis was too expensive, we settled for:

- def2-QZVPP - for the ISOL24 and C60ISO sets.
- def2-TZVPP - for the UPU23 set.
- def2-TZVP - for the two MOR reactions involving "ed24", "ed25", "pcy3", "pr24", "pr25" molecules

Furthermore, we have used *RIJCOSX* for approximating Coulomb and HF Exchange in our calculations and "TightSCF" Orca keyword for tight SCF convergences. For larger elements, when appropriate, we have used: def2-ECP effective core potentials (associated with the def2- basis set family).

S2. BREEDING OF "PRETTY TRANSFERABLE" BENCHSETS

In the main text, we formulate and motivate [see eq. (1) and eq. (last) and surrounding discussion] the unitless transferability of **A** to **B** and mean transferabilities of set **A**:

$$T_{\mathbf{B@A};p} = \frac{\mathrm{MAD}_{\mathbf{B@A};p} + \eta}{\mathrm{MAD}_{\mathbf{B@B};p} + \eta}\,, \qquad \bar{T}_p(\mathbf{A}) = \frac{1}{58} \sum_{\mathbf{B}\in\mathbf{TM+Org.}} T_{\mathbf{B@A};p} \tag{S1}$$

T measures the error on set **B** when optimized on **A** (**B@A**) versus its minimum error when optimized on itself (**B@B**). $\eta = 0.01$ kcal/mol regularizes results for small energies. $\bar{T}$ is the mean of this error over *all* 58 subsets of **TM+Org.**. Here, p indicates the number of parameters used in the optimization.

A random set involves 100 processes selected at random out of the 1506 processes of **TM+Org.**, and we create $N_{\mathrm{initial}} = 1000$ of these. $\bar{T}_7(\mathbf{rand}_R)$ will serve as our metric for breeding the pretty transferable sets, $\mathbf{PT}_K$ from $\mathbf{rand}_R$ – i.e. we use transferability on XYZ_7. We therefore also define $C_7 := N_{\mathrm{initial}}^{-1} \sum_{R=1}^{N_{\mathrm{initial}}} \bar{T}_7(\mathbf{rand}_R)$ to be the mean transferability obtained by chance, which we use as a normalizing factor.

Our goal is to construct 20 pretty transferable sets, via the following algorithm:

1. From the random sets, $\{\mathbf{rand}_R\}$, select the sets with the $N_{\mathrm{survive}} = 100$ lowest values of $\bar{T}_7$, to form a breeding pool, $\{\mathbf{breed}_B\}$.

2. Breed $\{\mathbf{breed}_B\}$ to create a single pretty transferable set:

   (a) Select the best [smallest $\bar{T}_7(\mathbf{breed}_B)$] set, $\mathbf{breed}_\alpha$, from the breeding pool, and another set, $\mathbf{breed}_\beta$, at random from the rest of the breeding pool;

   (b) Breed a new set, $\mathbf{breed}_\gamma$, that contains all N_S processes shared by $\mathbf{breed}_\alpha$ and $\mathbf{breed}_\beta$, and fills the remaining $100 - N_S$ processes by random selection from unshared elements of $\mathbf{breed}_\alpha$ and $\mathbf{breed}_\beta$;

   (c) Replace the worst [largest $\bar{T}_7(\mathbf{breed}_B)$] set in the breeding pool by $\mathbf{breed}_\gamma$, or leave the list unchanged if $\bar{T}_7(\mathbf{breed}_\gamma)$ is higher;

(d) Repeat from step 2a for up to $N_{\text{breed}} = 2000$ times, or until all $\bar{T}_7(\mathbf{breed}_B)$ are within $0.001C_7$ of each other.

3. Define $\mathbf{PT}_K = \mathbf{breed}_\alpha$, set $K \to K+1$ and repeat from step 1 (resetting the breeding pool each time) until 20 sets have been created.

The code `BreedTransferable.py` implements the above algorithm, while the code `PickBest.py` implements the second stage of T100's construction that is described in the main text. The pool of pretty transferable sets used to select T100 is cached (see `PickBest.py` for location) and read by `PickBest.py` to allow for reproducibility. All files are provided on the `github` repository [`XXX`] for this work.

S3. TRANSFERABILITY OF FUNCTIONALS TRAINED ON G21IP SET

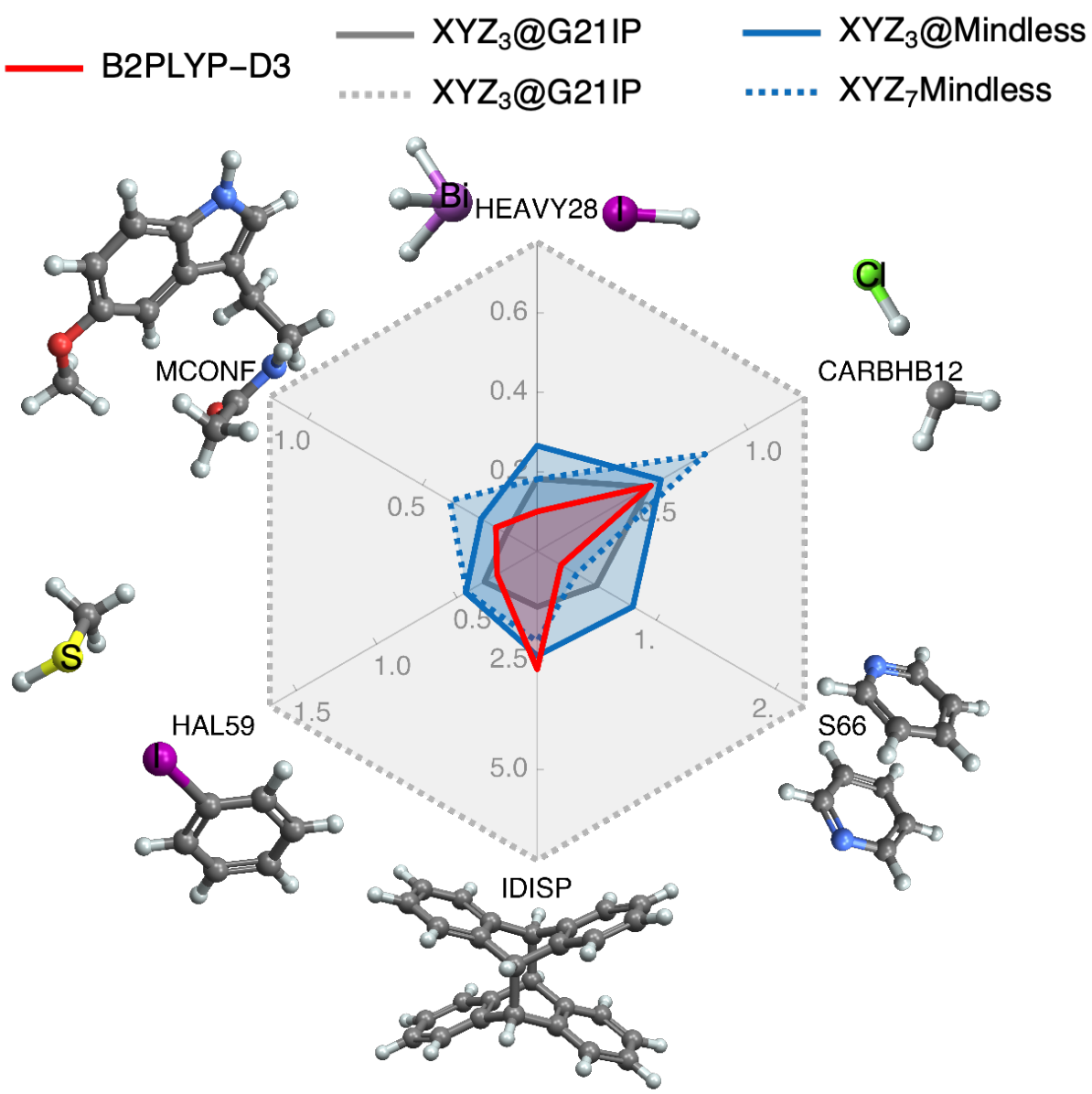

FIG. S1: Radial plots displaying MAD [kcal/mol] of selected functionals across different NCI subsets within the GMTKN55 database. The XYZ_3@G21IP functional, trained only on 21 ionization potentials, performs on par with or better than B2PLYP-D3, despite the former having no D3 dispersion correction. However, this transferability diminishes when extending from 3 to 7 parameters. Conversely, XYZ_N@Mindless functionals maintain consistent NCI performance as N transitions from 3 to 5.

S4. FURTHER DETAILS ON THE RESULTS IN FIGURE 1(A)

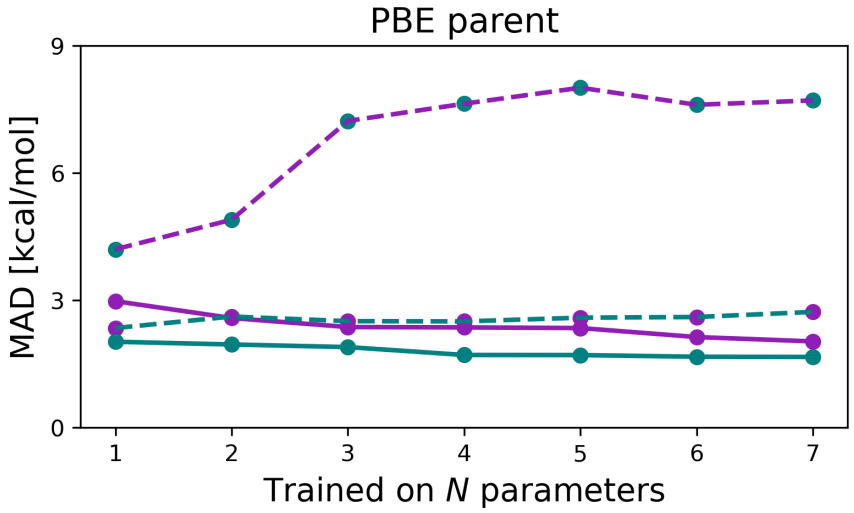

(a) PBE parent

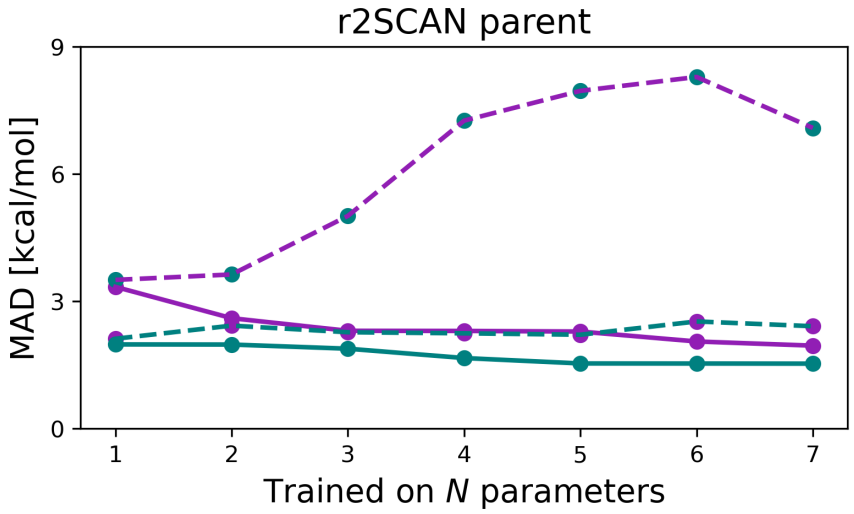

(b) r^{2}SCAN parents

FIG. S2: Same as figure 1(a), but with PBE and r^{2}SCAN parents, purple represents reactions energies (R), while teal color represents barriers (B): purple line with purple beads represents R@R, purple line with teal beads represents R@B, teal line with purple beads represents B@R, teal line with teal beads represents B@R.

S5. FURTHER DETAILS ON THE RESULTS IN FIGURE 1(C)

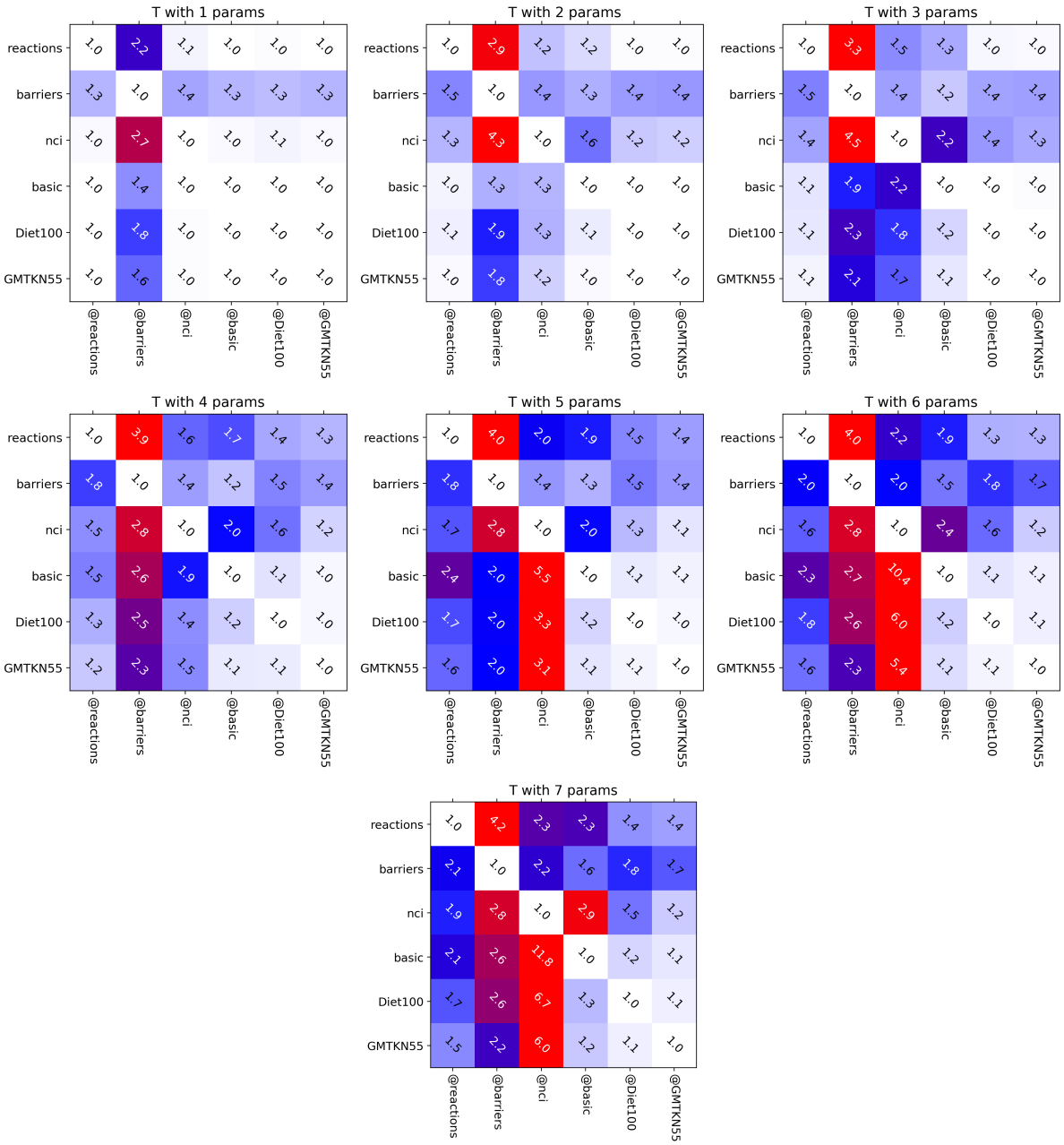

FIG. S3: Same as Figure 1(c), but for all number of parameters between 1 and 7.

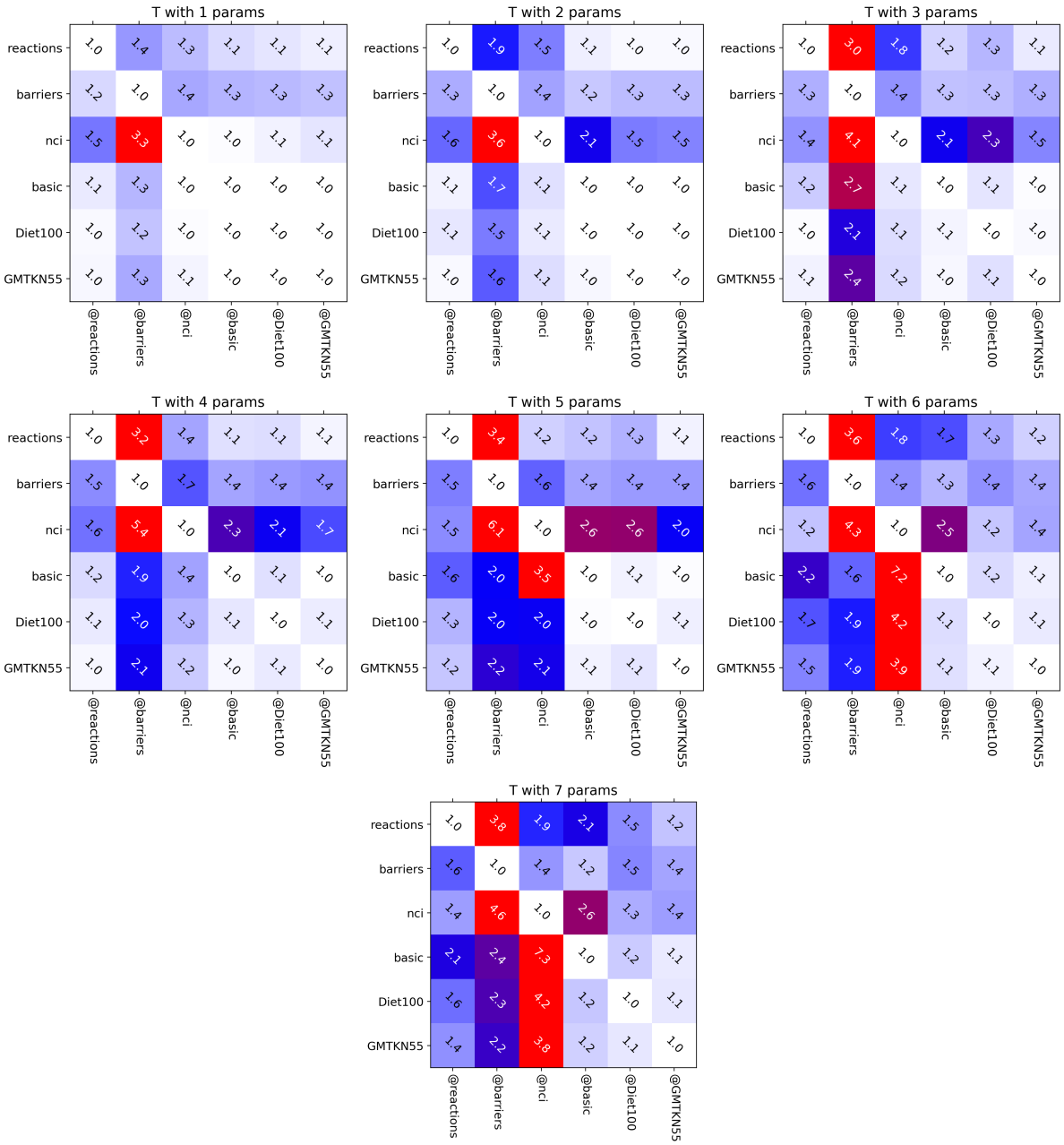

FIG. S4: Same as Figure S3, but for PBE parent.

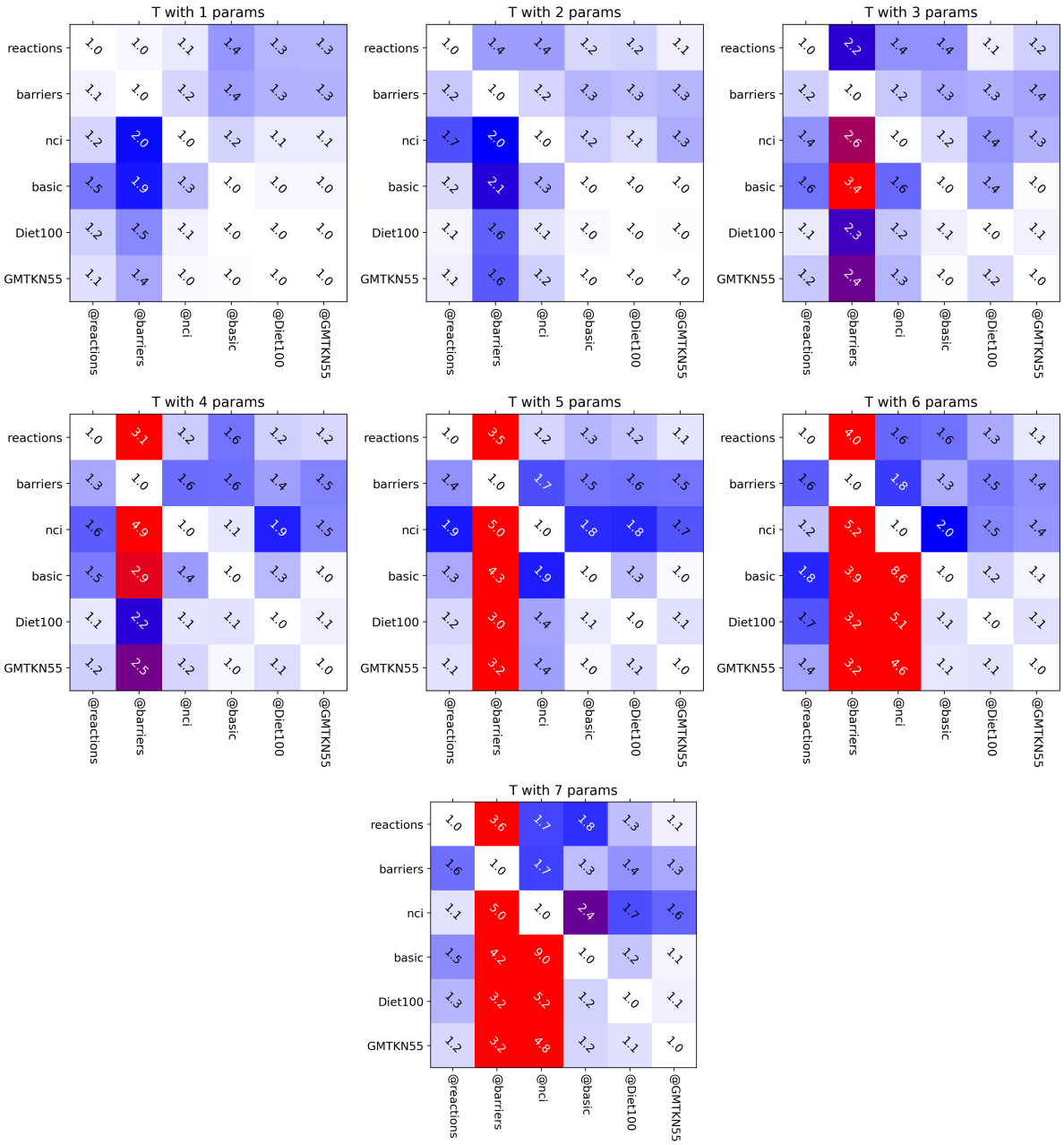

FIG. S5: Same as Figure S3, but for r^{2}SCAN parent.

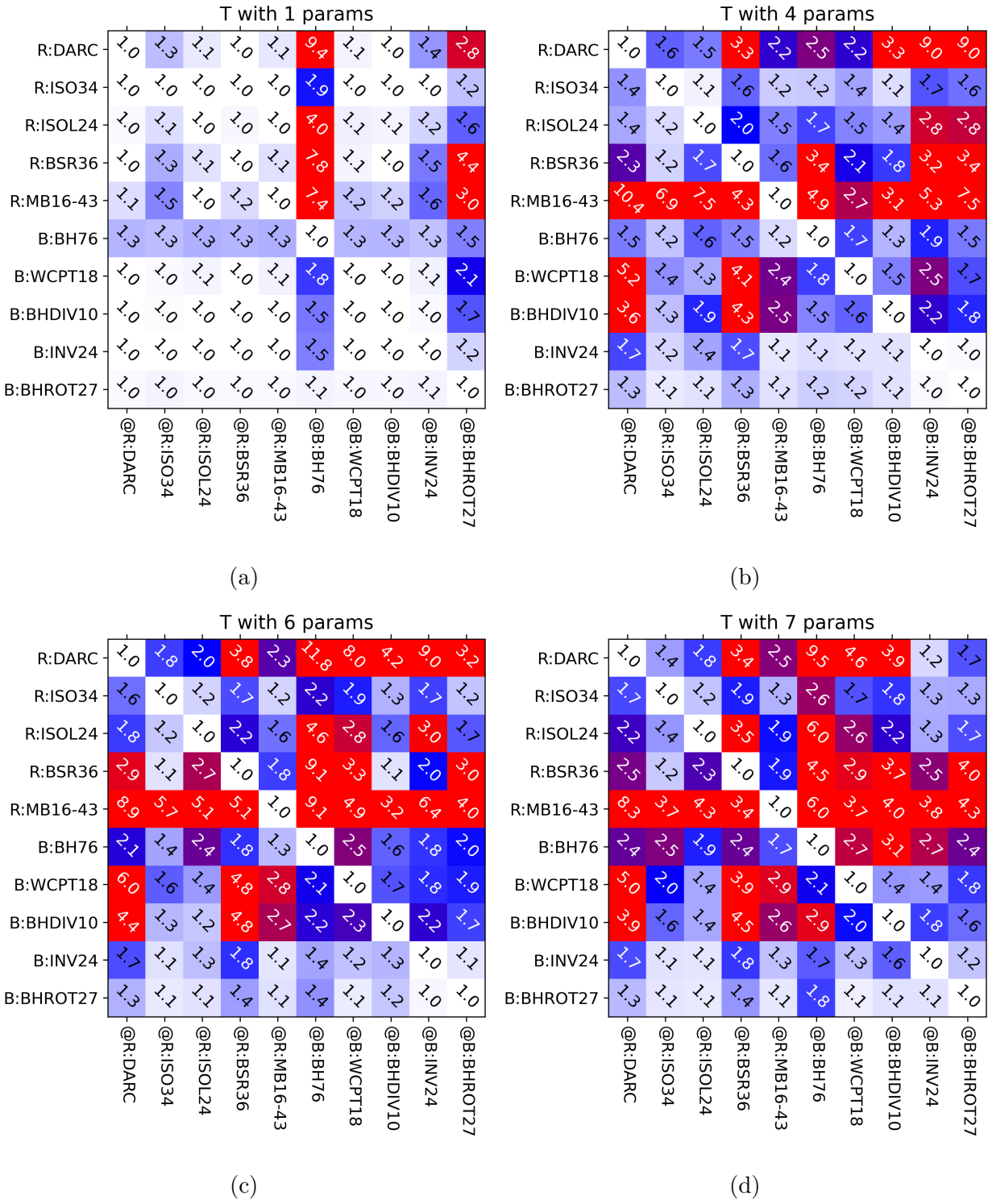

FIG. S6: Transferability matrices for reaction and barrier subsets of GMTKN55. **R@R** and **B@B** blocks of the matrices show the intra-reactions and intra-barriers transferability. **R@B** blocks show how barriers transfer to reactions. **B@R** blocks show how reactions transfer to barriers. η set to 1kcal/mol as the denominator of the transferability matrix for a single GMTKN55 subset becomes very small.

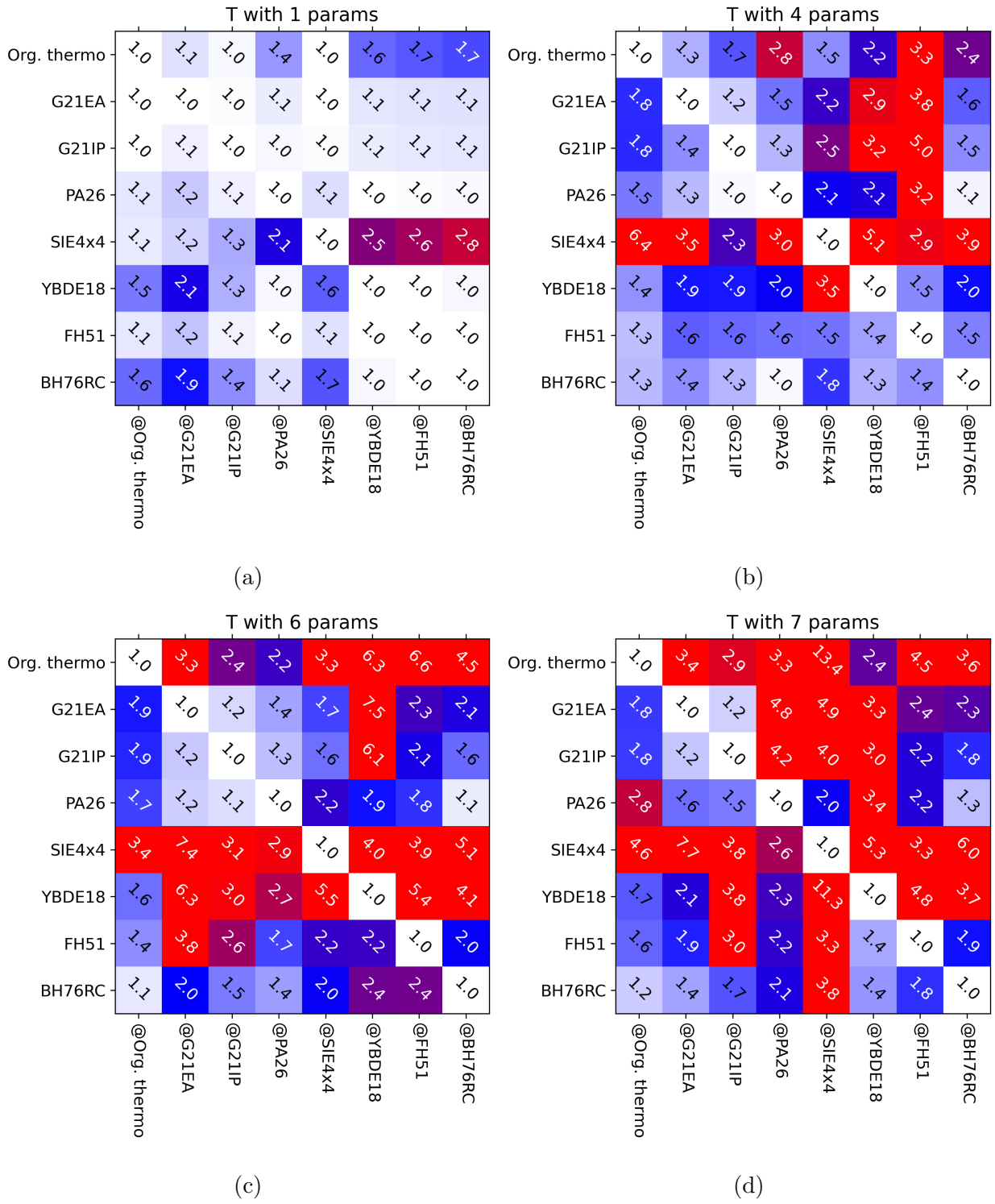

FIG. S7: intra-"Basic" Transferability matrices for the sets belonging to the "Basic" part of GMTKN55. η set to 1kcal/mol as the denominator when train only a single subset of GMTKN55 can get very small. "Org. Thermo" represents "W4-11" set.

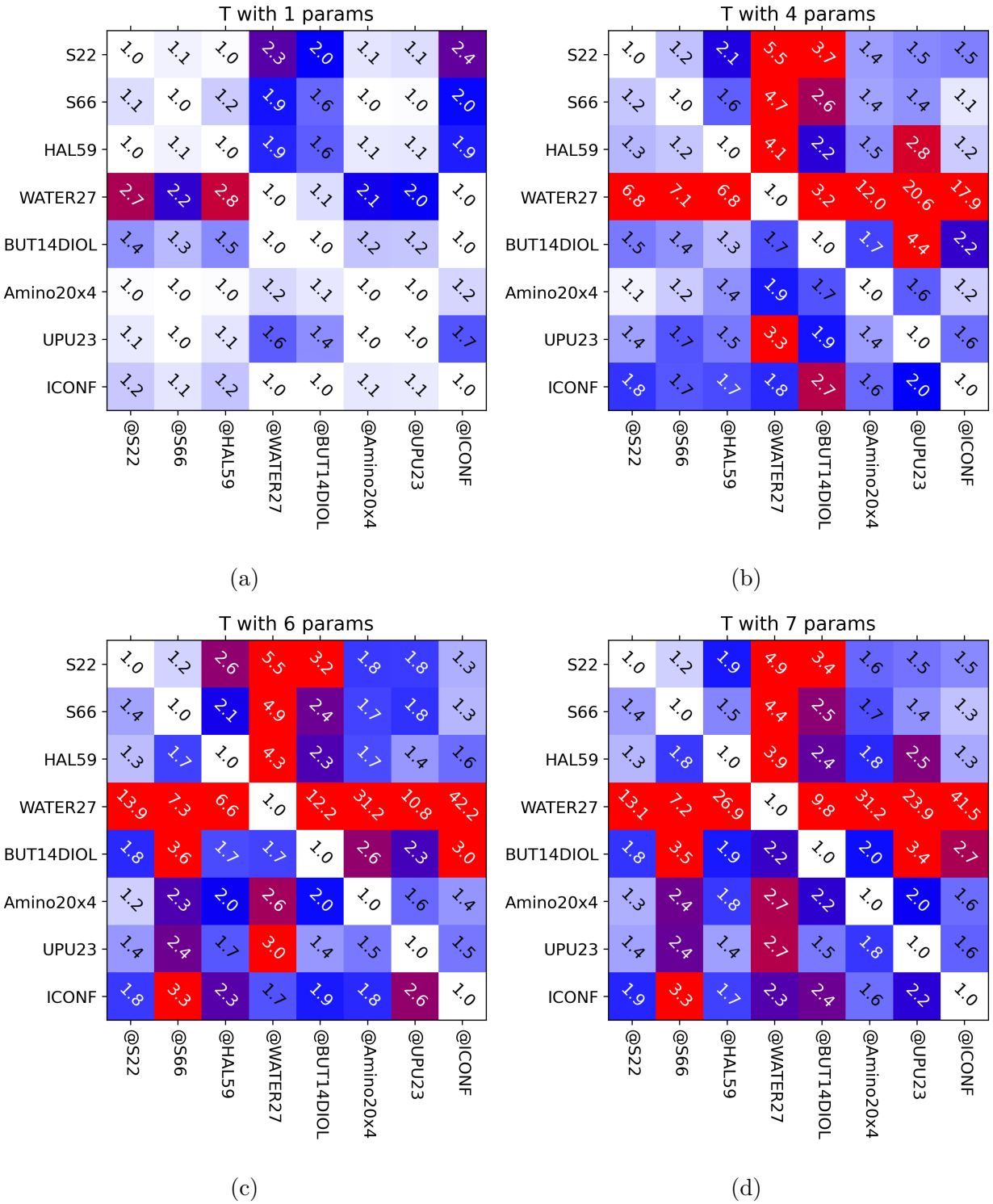

FIG. S8: Transferability matrices for the sets belonging to the "inter-NCI" part [first 4 sets] and "intra-NCI" [last 4 sets] of GMTKN55. η set to 0.1 kcal/mol.

S6. FURTHER DETAILS ON THE RESULTS IN FIGURE 2(A)

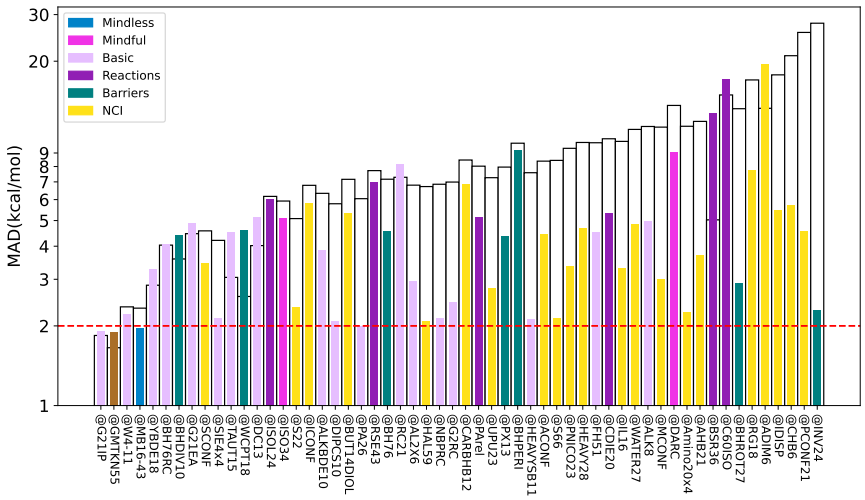

(a) PBE parent

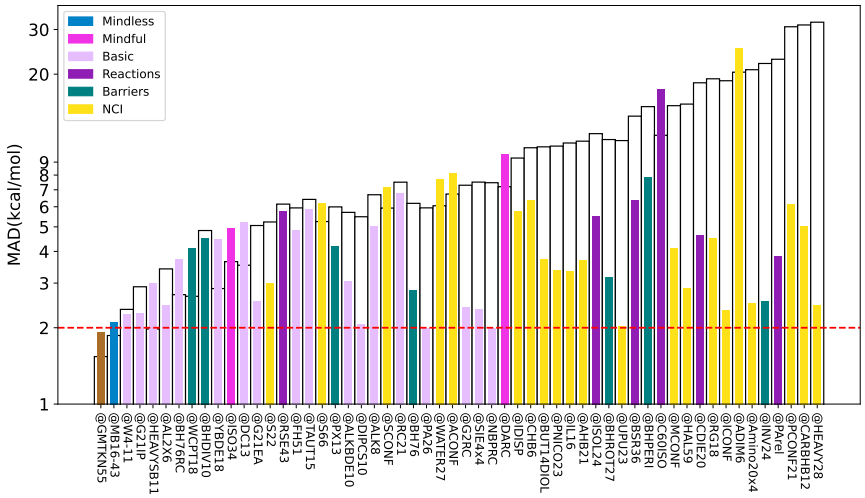

(b) r^{2}SCAN parent

FIG. S9: Same as figure 2(a), but with PBE and r^{2}SCAN parents.

The functional form used in Figure S10 is given by:

$$E_{\rm xc} = a_1 E_{\rm x}^{\rm HF} + a_2 E_{\rm x}^{\rm LDA} + a_3 E_{\rm x}^{\rm B88} + a_4 E_{\rm c}^{\rm LDA} + a_5 E_{\rm c}^{\rm LYP} + a_6 E_{\rm x}^{\rm MP2_{ss}} + a_7 E_{\rm x}^{\rm MP2_{os}} + a_8 E_{\rm c}^{\rm PBE} + a_9 E_{\rm c}^{\rm PBE} + a_{10} E_{\rm c}^{\rm r2SCAN} + a_{11} E_{\rm c}^{\rm r2SCAN} \quad \text{(S2)}$$

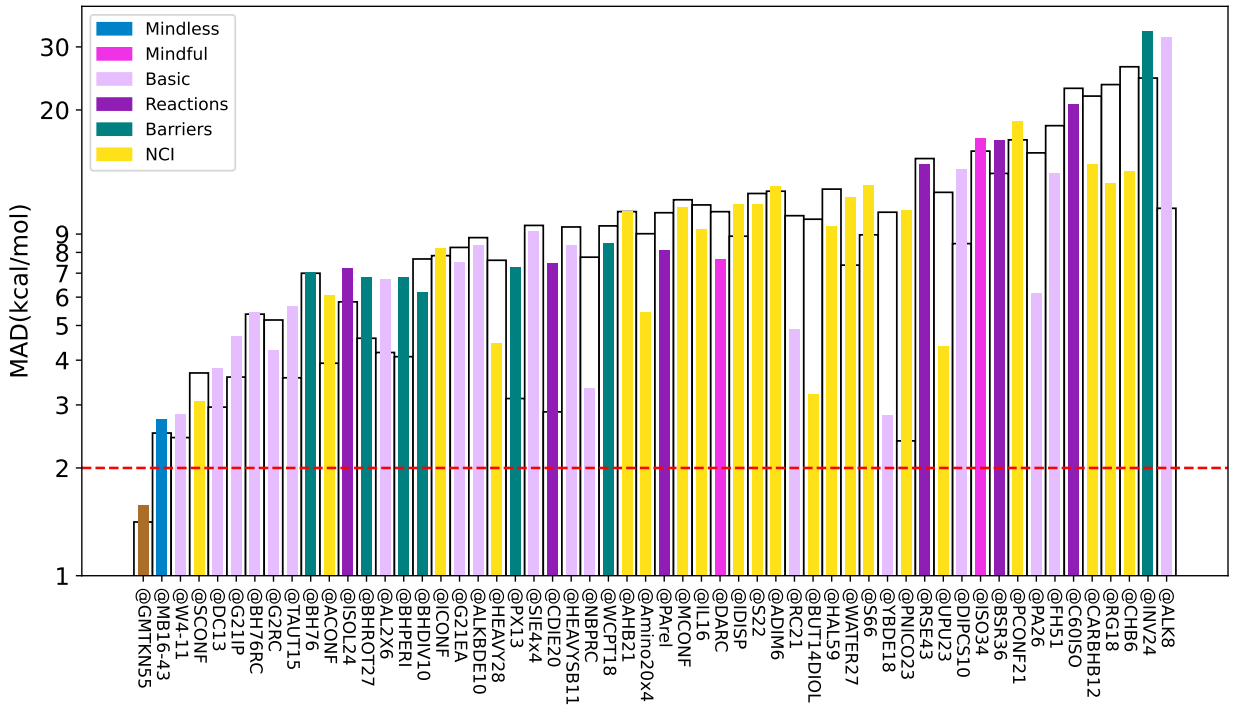

FIG. S10: Same as Figure 2a, but with double hybrids with 9 (DH9) and 11 (DH11) parameters. For DH11, we used functional form of Eq. S2. For DH9 we used the same form, but with a_{10} and a_{11} set to zero.

S7. DETAILS ON THE MINDFUL VS. MINDLESS ANALYSIS

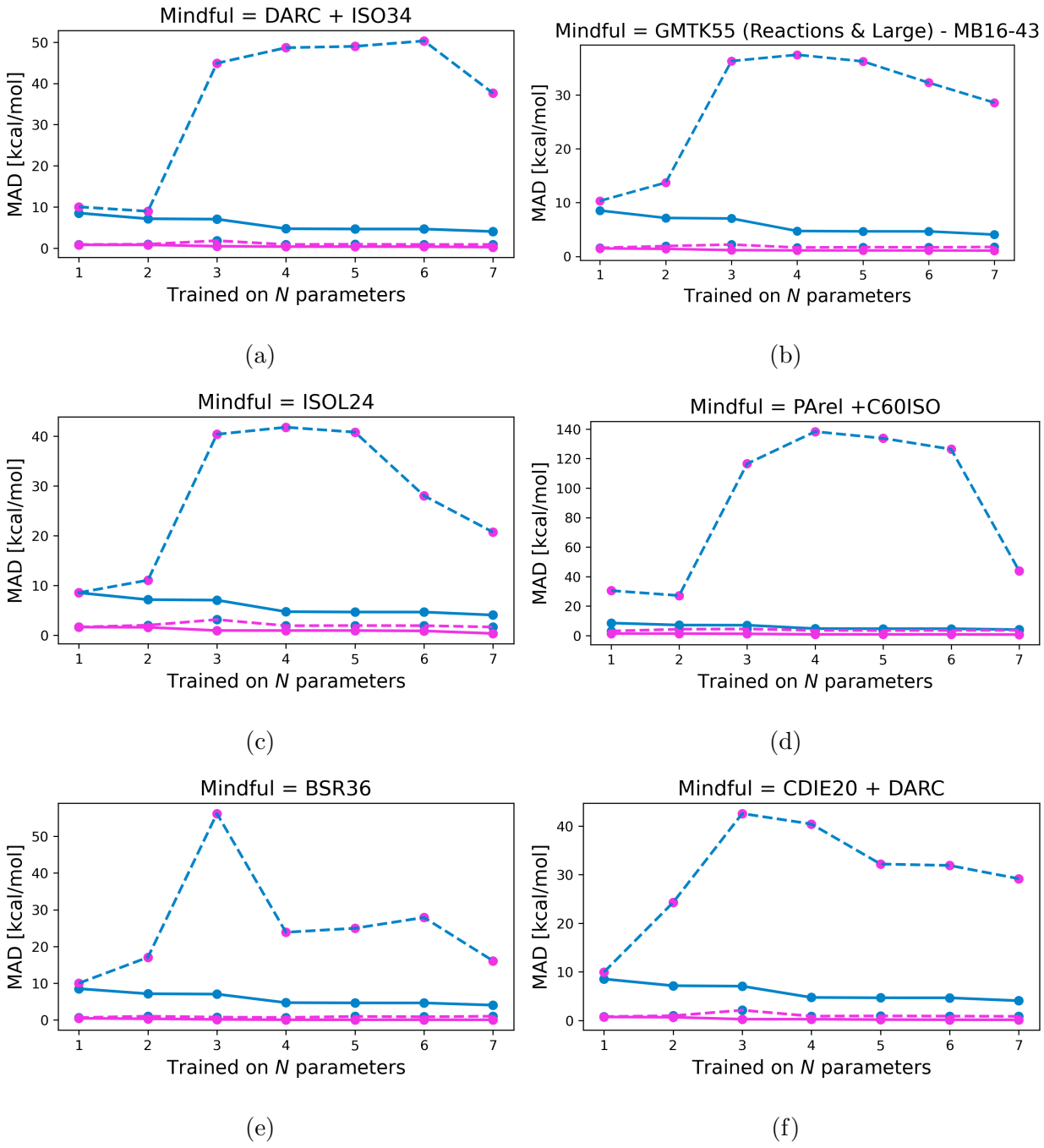

FIG. S11: Same as Figure 2(b), but with varying the "Mindful" dataset.

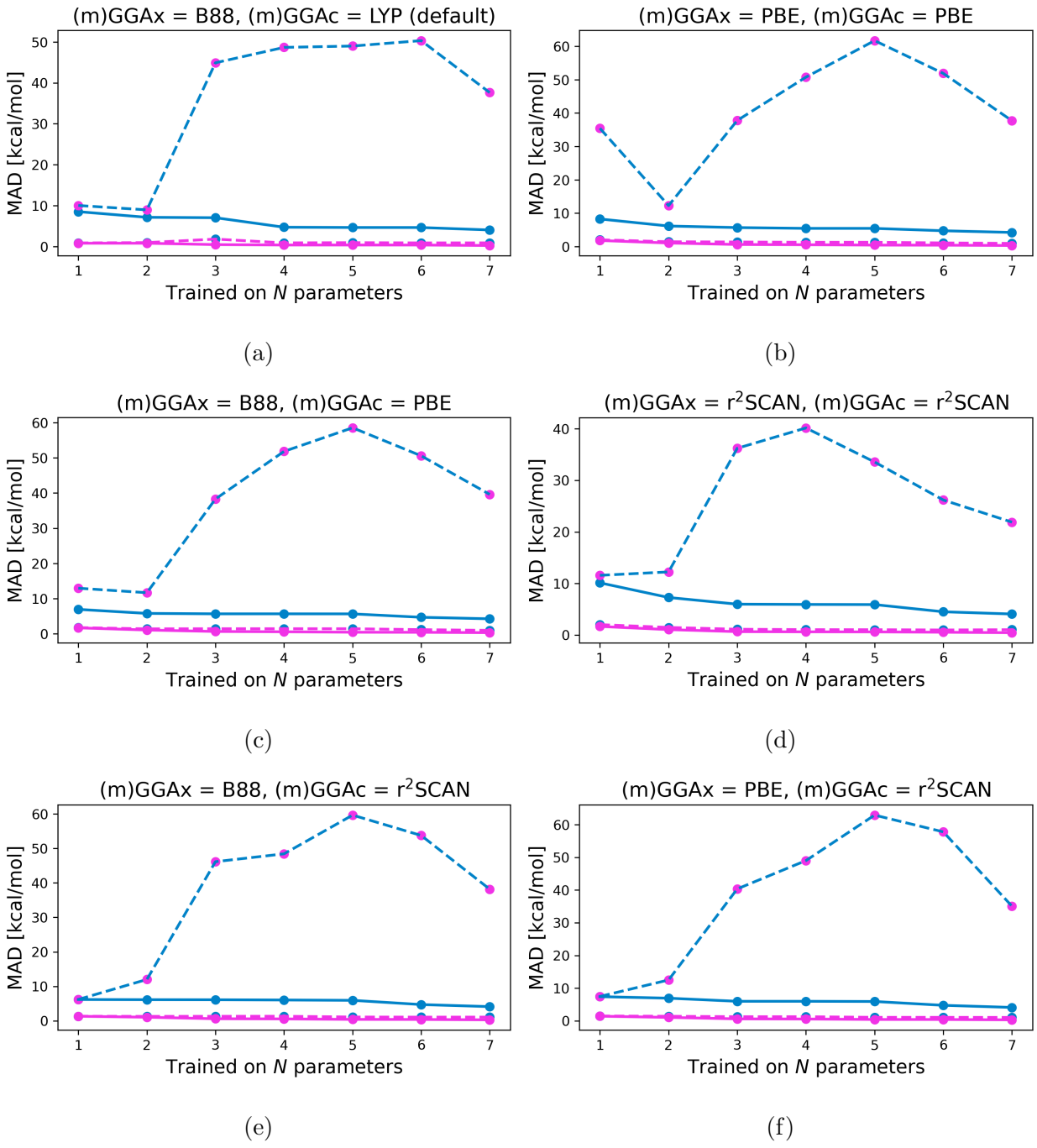

FIG. S12: Same as Figure 2(b), but with varying the (m)GGA parts in double hybrid forms.

S8. FURTHER DETAILS ON THE RESULTS IN FIGURE 3

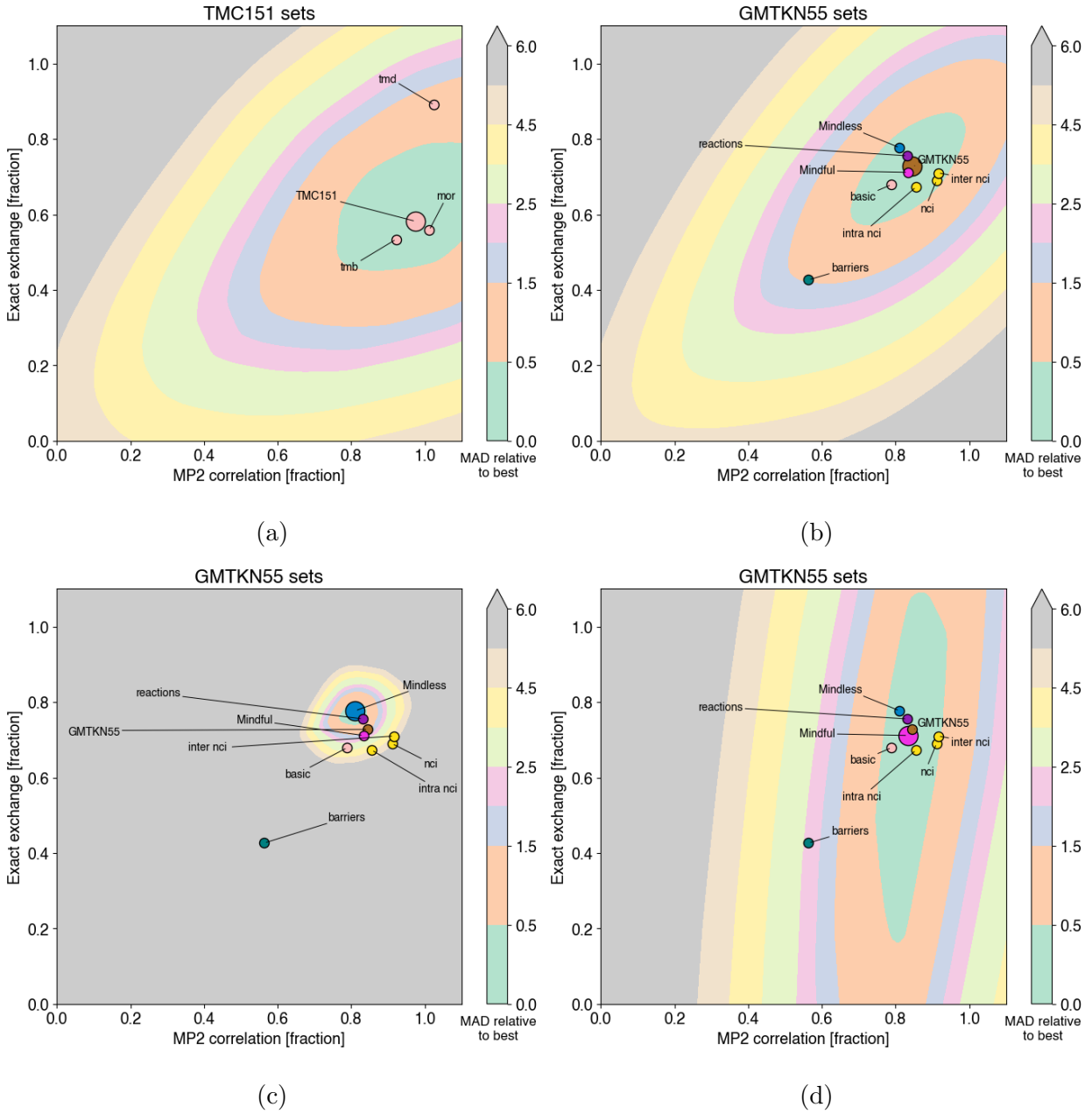

FIG. S13: Same as Figure 3, but with more datasets. 'MAD relative to best' in kcal/mol corresponds to the MAD dataset represented by the largest marker.

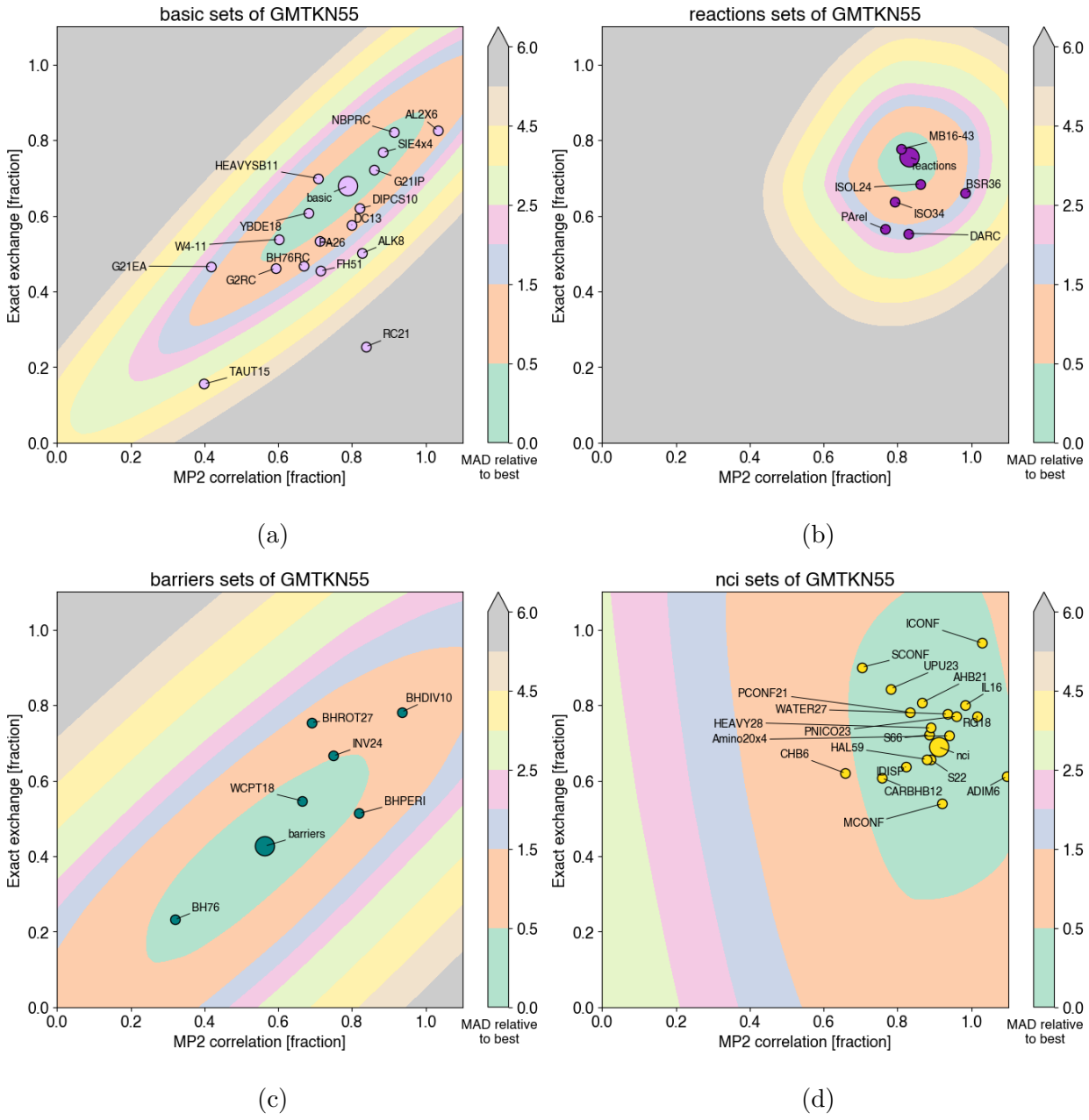

(a) (b)

(c) (d)

FIG. S14: Same as Figure 3, but with more datasets. 'MAD relative to best' in kcal/mol corresponds to the MAD dataset represented by the largest marker.

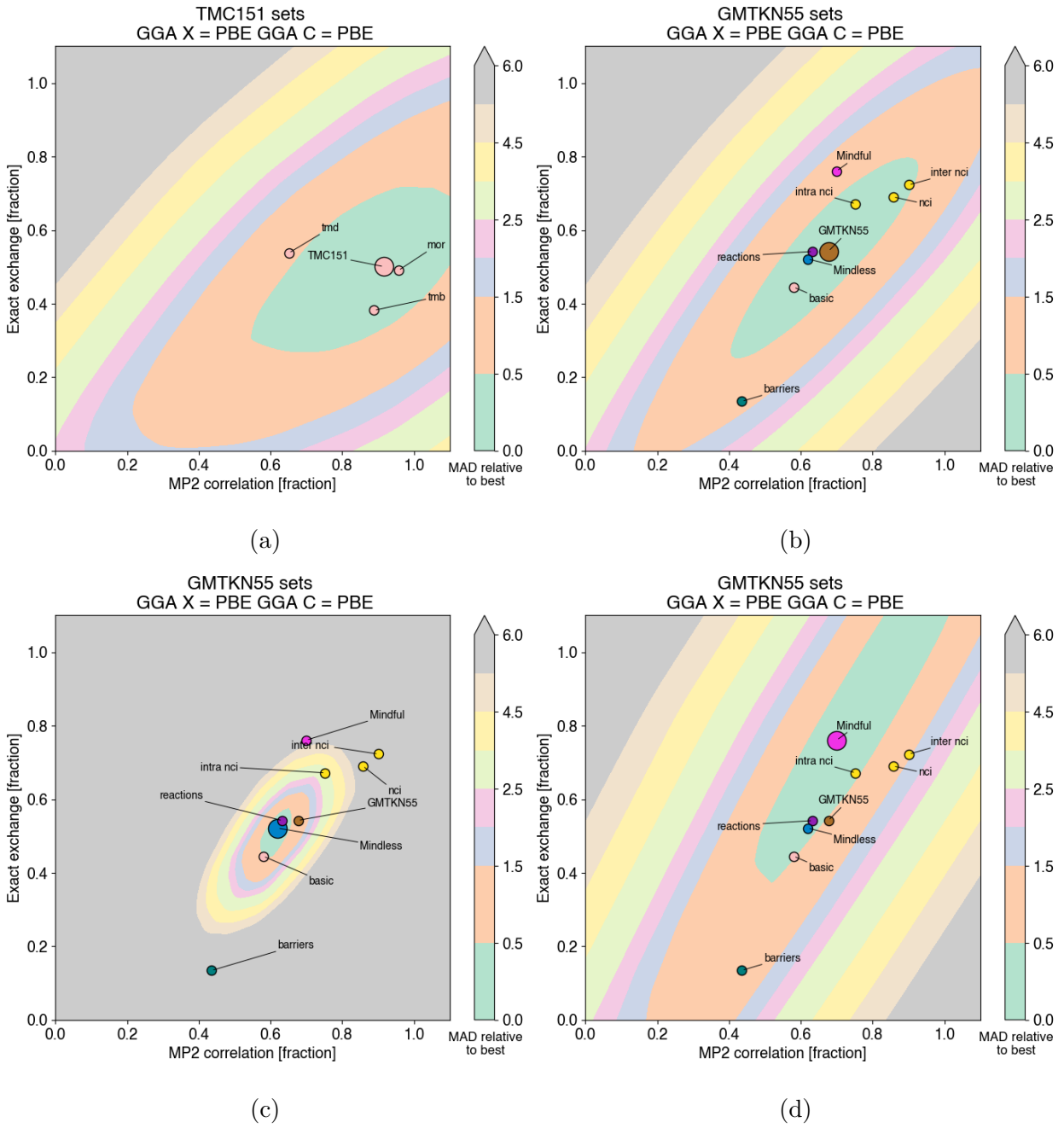

FIG. S15: Same as Figure S13, but with a double hybrid functional consisting of different (m)GGA parts. 'MAD relative to best' in kcal/mol corresponds to the MAD dataset represented by the largest marker.

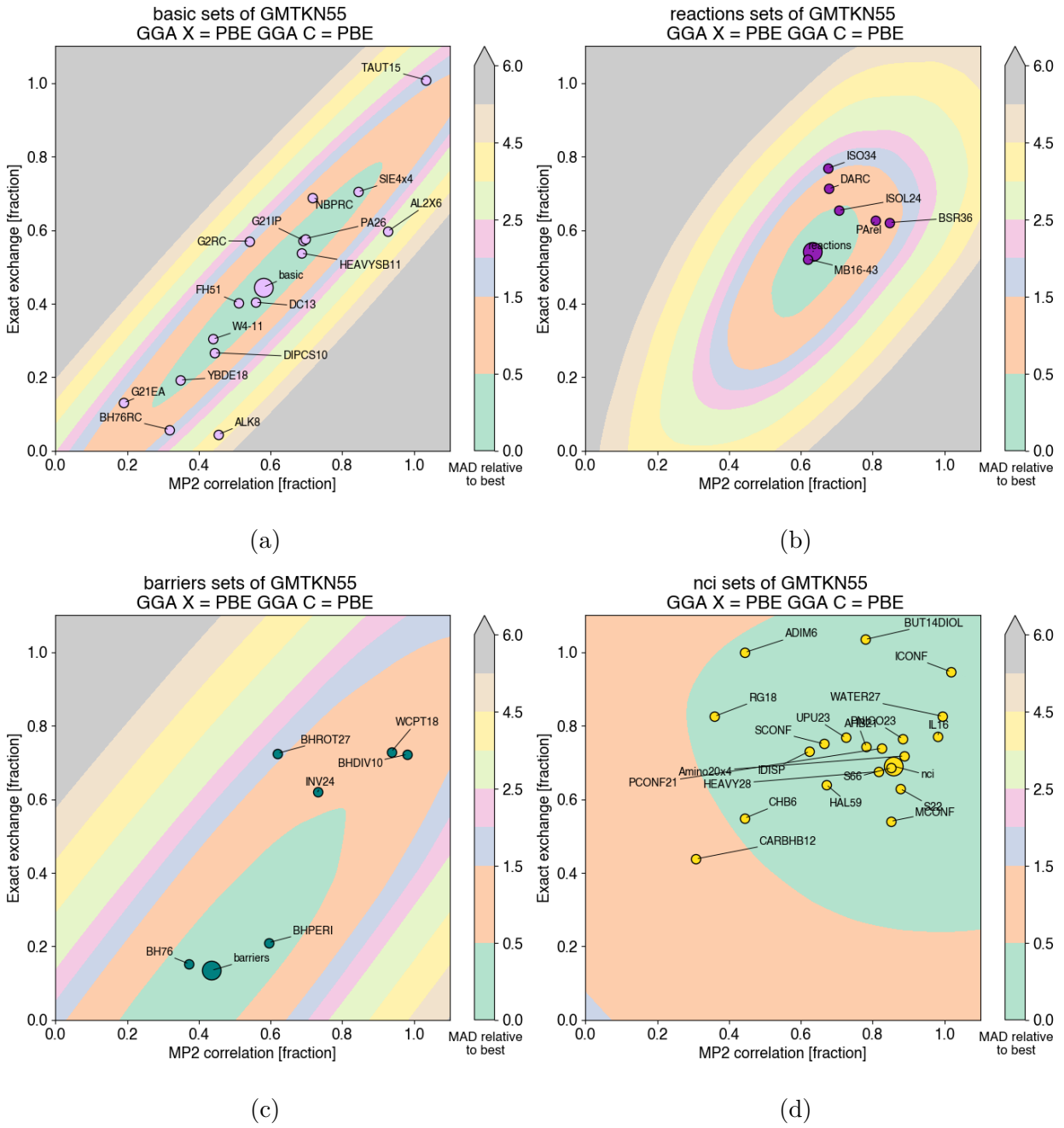

FIG. S16: Same as Figure S14, but with a double hybrid functional consisting of different (m)GGA parts. 'MAD relative to best' in kcal/mol corresponds to the MAD dataset represented by the largest marker.

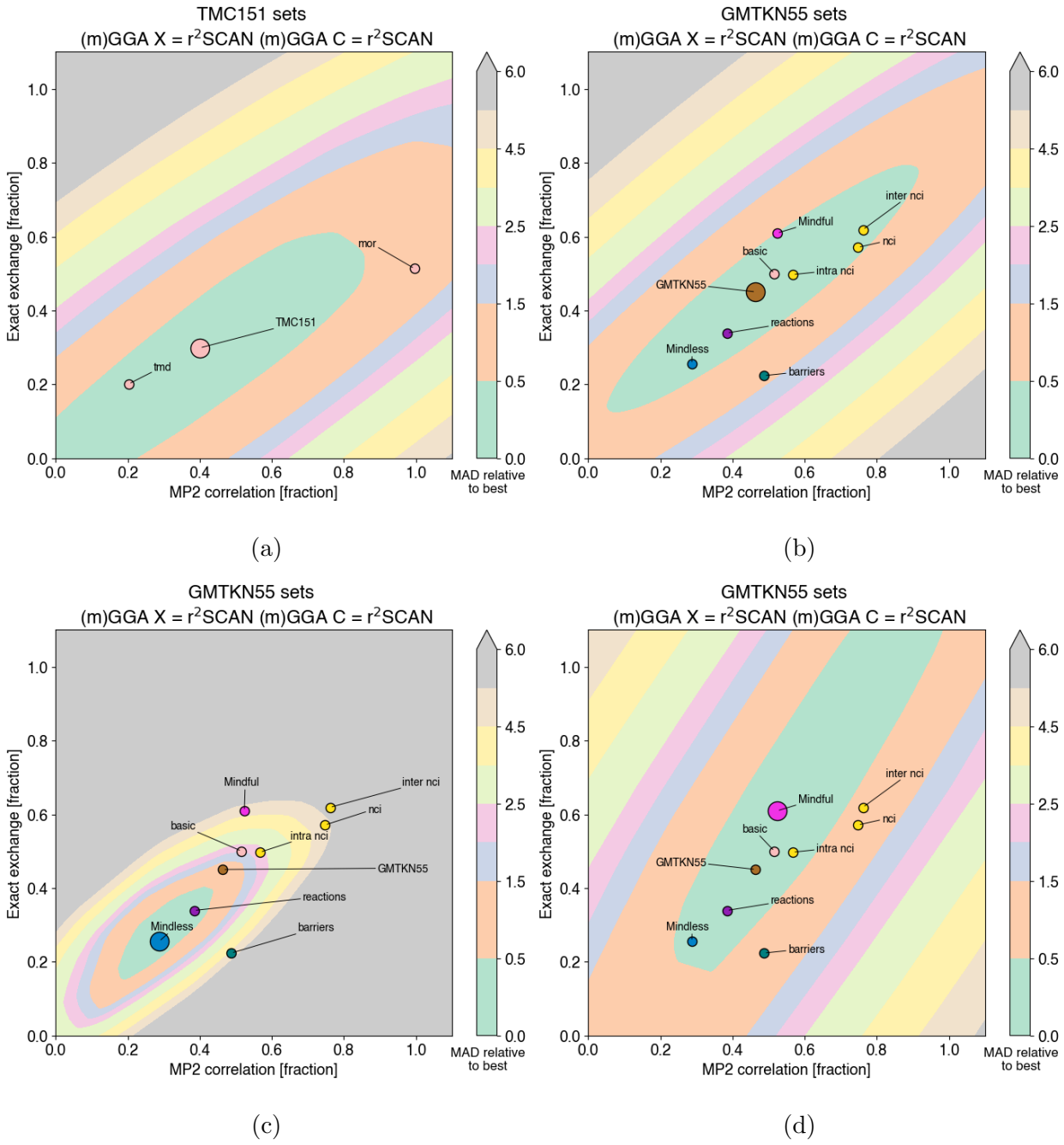

FIG. S17: Same as Figure S13, but with a double hybrid functional consisting of different (m)GGA parts. 'MAD relative to best' in kcal/mol corresponds to the MAD dataset represented by the largest marker.

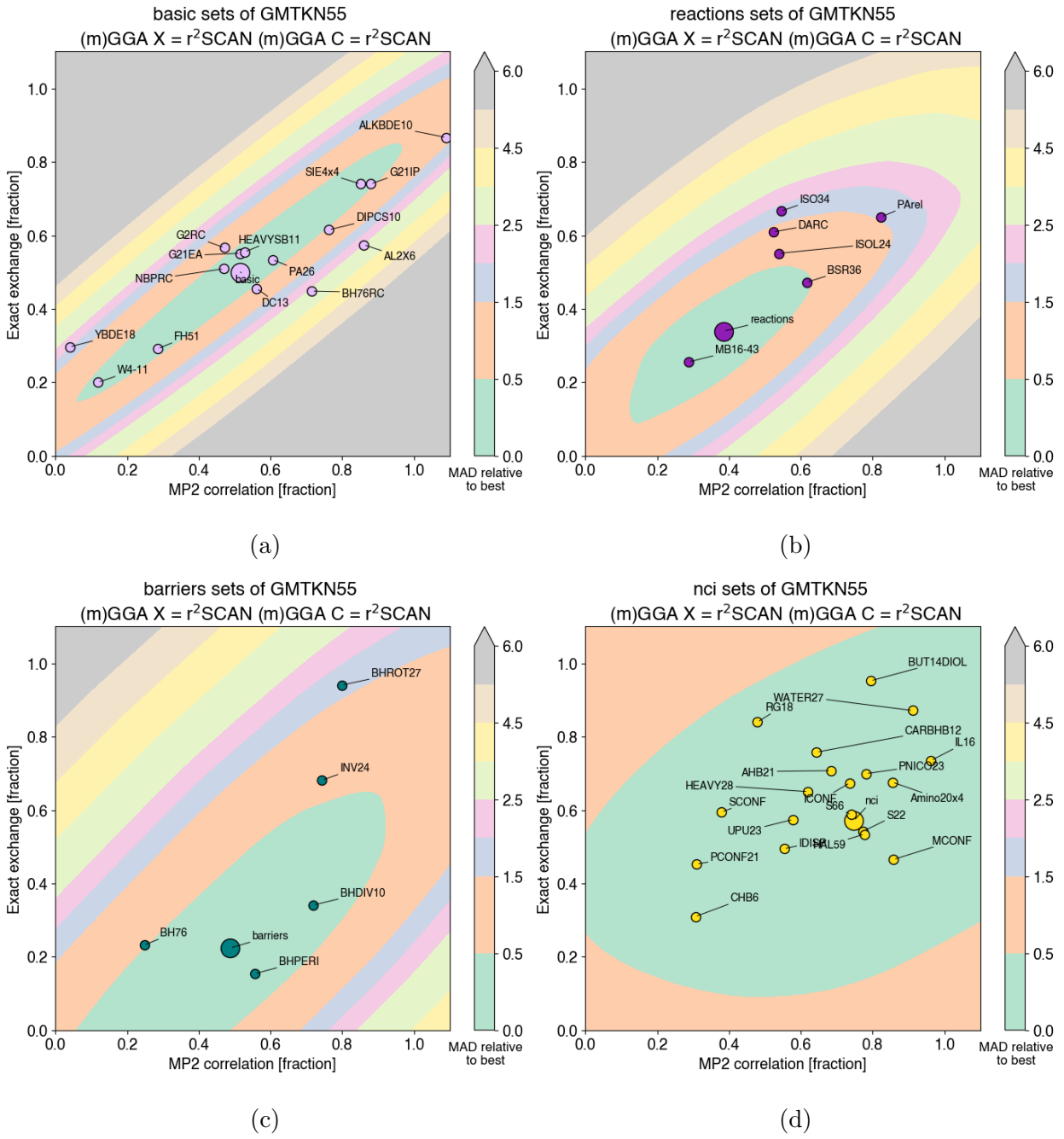

FIG. S18: Same as Figure S14, but with a double hybrid functional consisting of different (m)GGA parts. 'MAD relative to best' in kcal/mol corresponds to the MAD dataset represented by the largest marker.

S9. ADDITIONAL DETAILS FOR TM VS ORGANIC CHEMISTRY TRANSFERABILITY

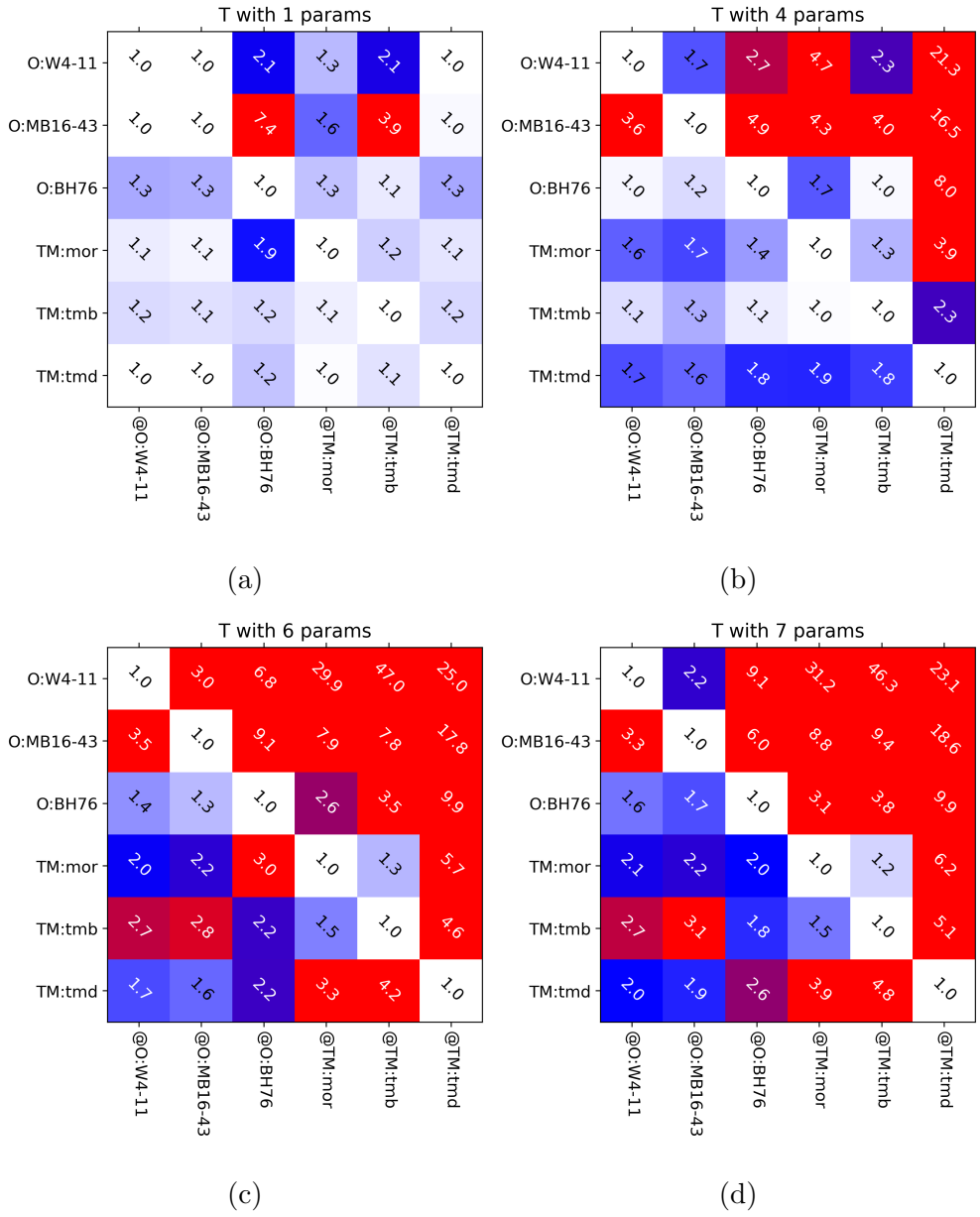

FIG. S19: Transferability matrices for selected TMC151 ["TM" label here] and GMTKN55 ["O" label here] sets. **O@O** and **TM@TM** blocks of the matrices shows the intra-TMC and intra-GMTKN55 transferability. **O@TM** blocks shows how transition metal sets transfer to organic ones. **TM@O** blocks shows how organic sets transfer to transition metal ones. η set to 1kcal/mol as the denominator when train only a single subset of GMTKN55 can get very small.

S10. ADDITIONAL RESULTS FOR SIE4X4 SET

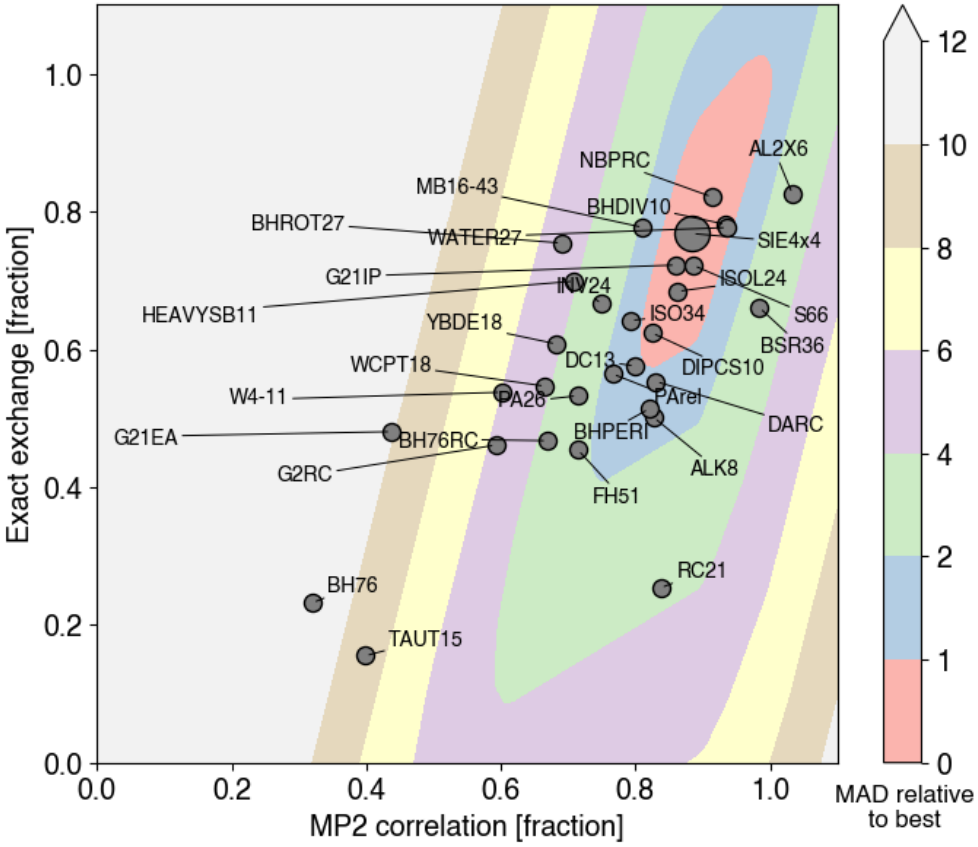

FIG. S20: Optimal values for the two-parameter model, XYZ_2 (markers) for selected GMTKN55 sets. Also shows the MAD (contours, kcal/mol) of SIE4x4 set as a function of the two parameters, relative to the optimal value.

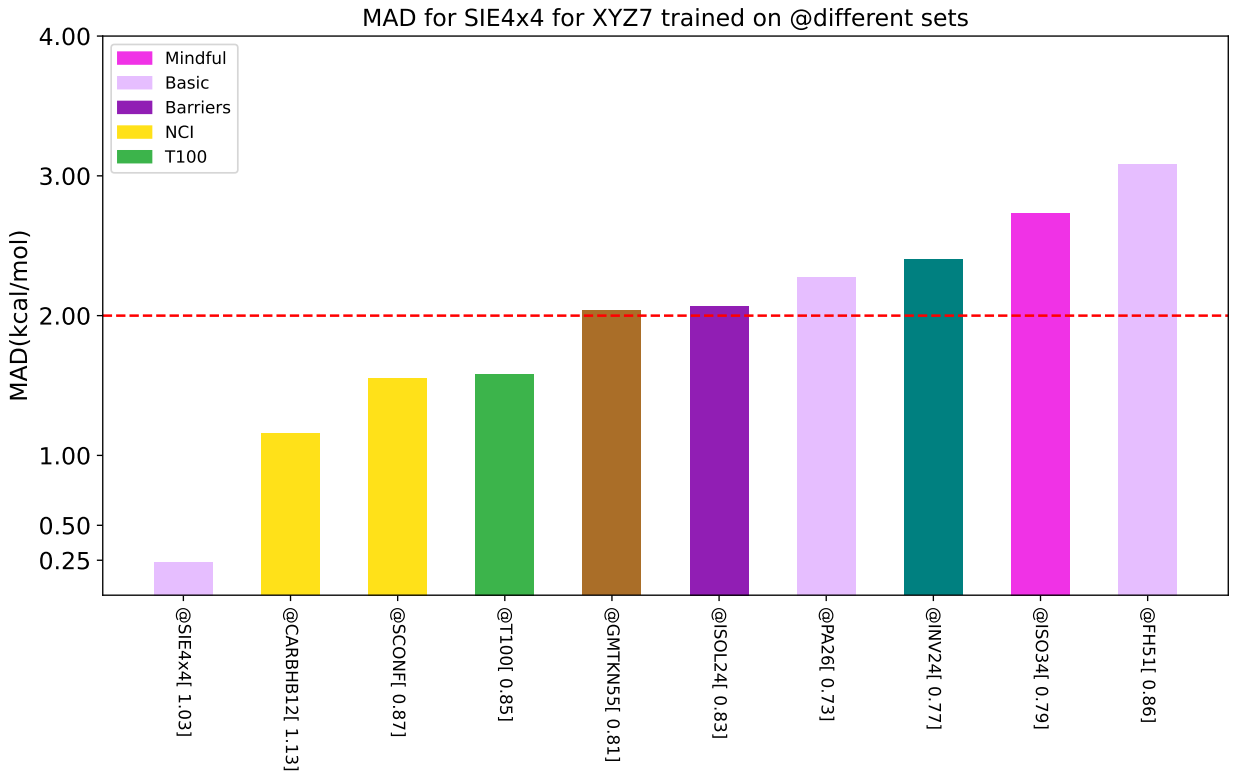

FIG. S21: Mean absolute deviation (MAD) for SIE4x4@set, where set is a subset of GMTKN55 for XYZ_7. 10 sets that give lowest SIE4x4@set MAD are shown. Below each bar, the name of @set is shown together with the fraction of exact exchange in XYZ_7 train on each individual set. For all shown bars (cases where SIE4x4@set MAD is the lowest), fraction of exact exchange is always greater than 73 percent.

S11. ADDITIONAL RESULTS FOR FIGURE 5 AND ACCURACY OF @T100-BASED FUNCTIONALS

REFERENCES

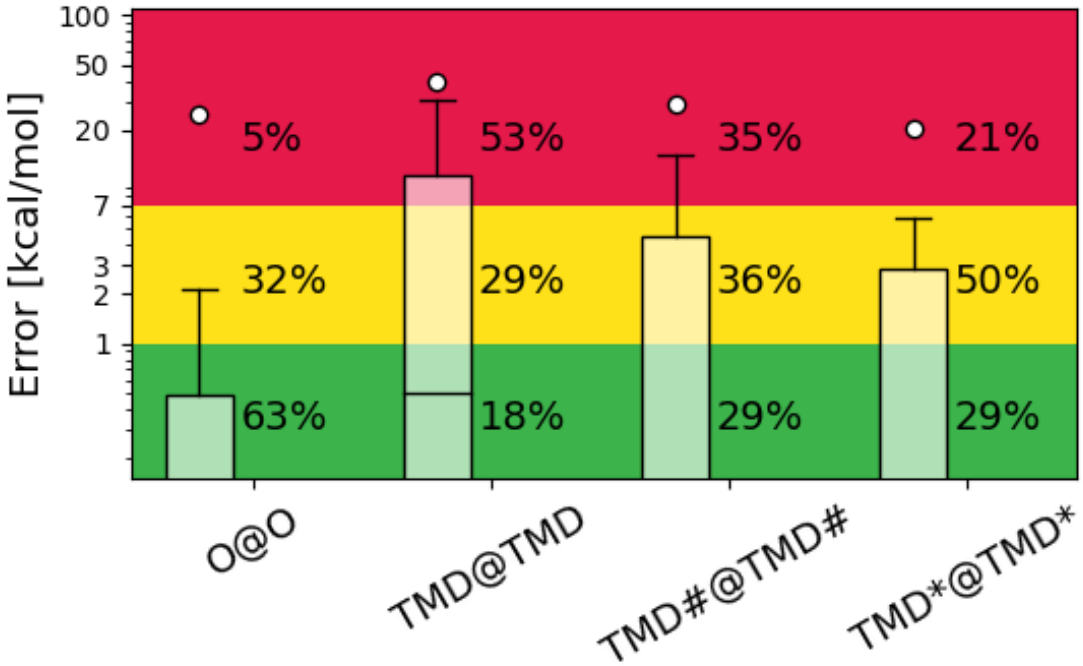

FIG. S22: Supplementary boxplots for Fig. 5. O: GMTKN55; TMD: TMDiff; TMD#: Subset of TMD60 with available CCSDTQ data and matching MOR and TMB reactions in TMDiff; TMD*: TMDiff minus spin-contaminated reactions, defined as those with at least one species with HF's $\langle S^2 \rangle$ deviating from its ideal value by more than 10 percent and by more than 0.05. TMD, TMD#, TMD* have 68, 28, 34 reactions, respectively.

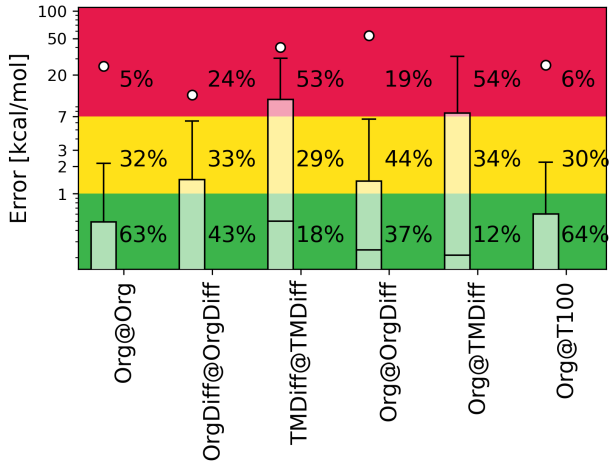

(a) same as Fig. 5, but with errors given in boxplots

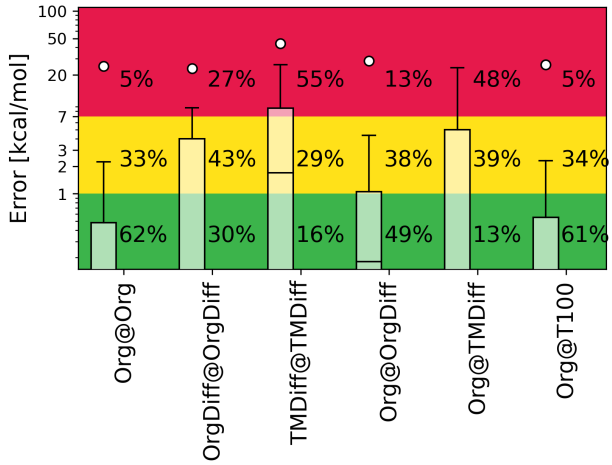

(b) same as panel (a), but with PBE parent

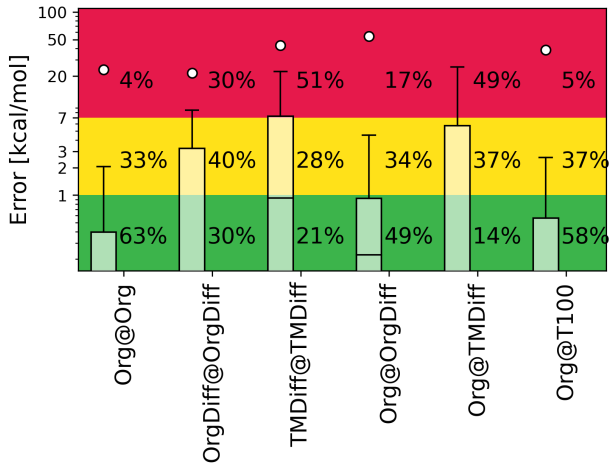

(c) same as panel (a), but with r^{2}SCAN parent

FIG. S23: Supplementary boxplots for Fig. 5

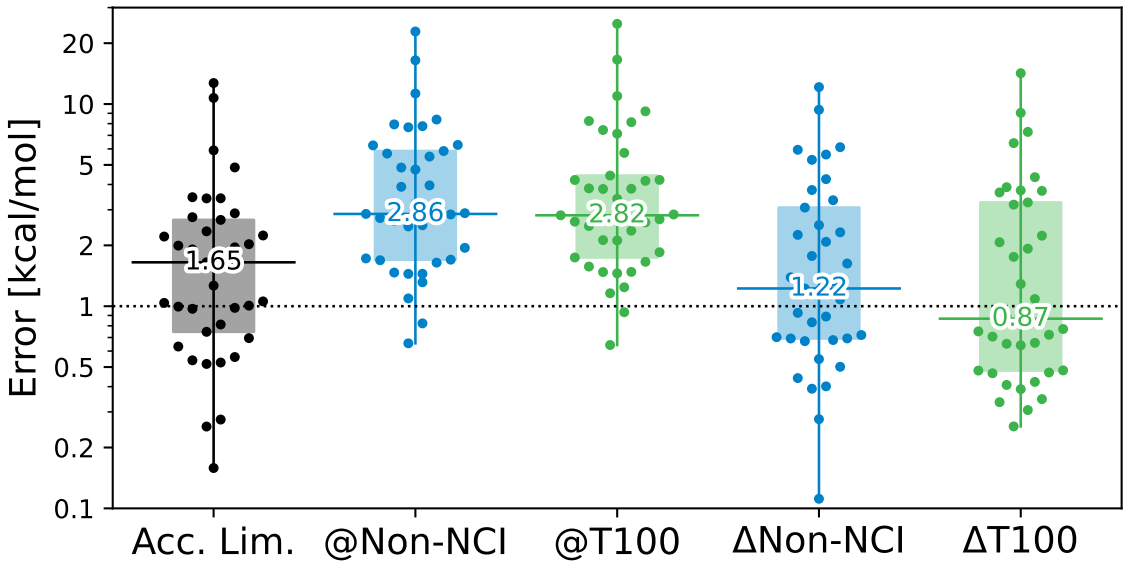

FIG. S24: Transferability energy (same as Fig. 4) with the B3LYP functional form (still with HF orbitals), for the non-NCI subsets of GMTKN55. The black "Acc. Limit" displays MADs for each non-NCI subset using "@Self" for training. Comparisons are drawn with results trained on the complete non-NCI GMTKN55 set (blue bar) and the T100 set (green bar). The final two Δ bars represent the difference between the full dataset and "@Self" training (blue minus black) and T100 and "@Self" training (green minus black). The non-NCI portion of GMTKN55 is selected due to B3LYP's inability (lacking MP2 admixture or dispersion corrections) to capture, dispersion interactions, which are crucial for simulating NCIs.